

Robust maximum power point tracking control for photovoltaic system based on second order sliding-mode

A. Fezzani¹, N. Bouarroudj², S. Drid³, L. Zaghba⁴

^{1,2,4}Unité de Recherche Appliquée en Energies Renouvelables, URAER, Centre de Développement des Energies Renouvelables, CDER, Algeria

³LSPIE, Laboratory, Electrical Engineering Department, University of Batna 2, Algeria

Article Info

Article history:

Received Feb 4, 2020

Revised Feb 19, 2020

Accepted Mar 20, 2020

Keywords:

dSPACE controller board

Maximum power point

Shell Solar S75 PV

Sliding mode control

Super twisting algorithm

ABSTRACT

This paper proposes a control approach of a maximum power point of a photovoltaic (PV) system using the second order sliding mode approach. The main objective of the proposed paper is to track the maximum power point (MPP) using super twisting algorithm (STA) with a one-loop control method and augment efficiency of the output power system. The structure of a proposed approach is simple and robust aging the atmospheric changes. Such control approach solution has several advantages such as simple implementation, robustness; reduce the chattering phenomenon and good dynamic response compared to traditional first-order sliding mode control algorithm. The controller circuit adapts the duty cycle of the switch electronic device of the DC/DC converter to search maximum power point tracking as a function of evolution of the power input. The effectiveness and feasibility of the proposed control are verified by simulation in MATLAB/Simulink environment and dSPACE-based hardware in loop platform.

This is an open access article under the [CC BY-SA](https://creativecommons.org/licenses/by-sa/4.0/) license.



Corresponding Author:

Amor Fezzani,

Unité de Recherche Appliquée en Energies Renouvelables, URAER,

Centre de Développement des Energies Renouvelables,

CDER, 47133, Ghardaïa, Algeria.

Email: amorfezzani@yahoo.fr

1. INTRODUCTION

Solar energy represents a viable energy alternative for the production of electricity since the latter is a renewable source, both clean, unlimited and with a very low level of risk [1-3]. However, a major challenge in using an energy generated by photovoltaic systems is to undertake its nonlinear output characteristics, which depend of solar insolation and temperature module. An important in the operation of a PV generator is to reach the maximum output power by means of continuously correcting the PV array operating point for the given conditions. The main objective of maximum power point tracking (MPPT) method is to automatically obtain an optimal MPP operation under real outdoor conditions.

Several MPPT techniques have been developed in literature. Some of the popular schemes are the Open-circuit voltage method [4], incremental conductance methods [5, 6] and perturb and observer (P&O) methods [7]. In the open circuit voltage technique, in order to calculate V_{OC} , power inverter should be turned off for a few seconds. Thus, at each calculation, some power is lost. Another drawback of this technique is that it cannot track MPP at the effects of the irradiation changes. The P&O is most widely due to its simplicity and easily implemented. However, P&O have major disadvantage because he does not consider the effects when the atmospheric conditions change rapidly [8, 9]. Incremental conductance can perform MPPT faster under different atmospheric conditions with high accuracy but it increase system complexity.

There are also other algorithms such as the artificial neural network technique (ANN) [10], particle swarm optimization (PSO) [11], fuzzy logic approach [12] and adaptive neuron-fuzzy technique [13]. The algorithms should have a high performance to MPP track. However, their implementations are expensive and complex [14]. In that sense, robust Sliding Mode Control is an interesting solution for non-linear control derived from variable structure control (VSC) system theory and developed by UTKIN [15]. Such controller has many advantages for example, simple implementation, well dynamic response and good robustness.

VSC technique for PV application was proposed and evaluated by numerical study in [16]. Further study was also suggested in [17-19], however, these approaches required current or a voltage reference for control law synthesis and can lead to a lack of robustness to operation conditions. In [20] there is no necessity to have a reference value since the sliding surface guarantees the MPP when it is equal to zero. But the chattering phenomenon, originated by the interaction between parasite dynamic and finite-frequency switching control is the main disadvantages of this techniques of control [21, 22]. To minimize chattering phenomena some methods were proposed [23-25]. To preserve the main advantages of the sliding mode technique and to reduce the chattering phenomenon, a novel class of SMC algorithm, called second-order SMC algorithm (2-SMC) has been proposed in [26, 27].

In Saharaoui et al. [28], a 2-SMC was applied with a two-loop control approach. A simulation study by Yatimi et al., [29] presents a robust sliding mode method for a photovoltaic energy storage system. Another method to track the MPP given in Mojallizadeh et al., [30], the proposed scheme is based on the second-order fuzzy sliding mode control law of photovoltaic power generation systems with a two-loop control. Moreover, in Kckaou et al., [31] offer a second-order sliding MPPT control for photovoltaic application. The main objective of this work is the use one loop technique of 2-SMC based on super twisting algorithm to extract MPP, reduce the chattering phenomenon and real-time implementation study under different operating scenarios. The control circuit use an algorithm to adapt the duty cycle of the switch control of the DC-DC converter to search MPP tracking as a function of evolution of the power input. This paper consists of four sections, including the introduction. Section 2 materials and methods, and section 3 results and discussion. Finally, the conclusions of the study are given in section 4.

2. MATERIALS AND METHODS

2.1. Photovoltaic systems

2.1.1. Mathematical modelling and simulation

The physical behaviour of the panel has conventionally been studied by representing it as an equivalent electrical circuit composed of linear and non-linear components. Solar cell (SPV) is the elementary component which converts the energy of light directly into electricity by the PV effect. PV arrays are built up with combined series/parallel combinations of SPV [32, 33]. Each cell is typically a p-n junction. There are various circuit schemes for a photovoltaic cell in literature. A single diode model is considered as the equivalent photovoltaic cell in the present paper [33]. The basic model for a photovoltaic cell is show in Figure 1.

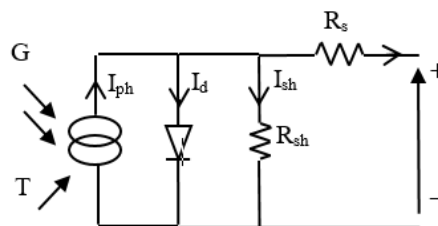


Figure 1. Simplified equivalent circuit PV model

The one diode equivalent circuit determines the I-V characteristic of the cell is described by the following (1):

$$I = I_{ph} - I_0 \left[e^{\frac{V+IR_s}{V_t}} - 1 \right] - \frac{V+IR_s}{R_{sh}} \quad (1)$$

where I is the cell output current (A), V is the cell output voltage (V), I_{ph} is the photocurrent, function of the irradiation level (G) and junction temperature, I_0 is the reverse saturation current of diode, $V_t = aKT_c/q$ is the thermal voltage, q is the electron charge ($1.602 \times 10^{-19}C$), K is the Boltzmann constant ($1.38 \times 10^{-23}J/K$), a is

the ideal factor, T_c is the temperature of the cell, R_s and R_{sh} the serial and parallel resistances respectively and I_d , called diode (D) current or dark current. The photocurrent I_{ph} can be assessed with the (2):

$$I_{ph} = I_{STC} \frac{G}{G_{STC}} [1 + \alpha(T_c - T_{c,STC})] \tag{2}$$

where I_{STC} is the short circuit current at standard test condition (STC), while G_{STC} and $T_{c,STC}$ are the irradiation and temperature of the PV cell at STC, respectively; α is the current temperature coefficient. With regard to the reverse saturation current I_0 parameter, its value changes with cell temperature at STC conditions and can be found by using the following (3).

$$I_0 = I_{rs} \left(\frac{T_c}{T_{c,STC}} \right)^3 e^{qE_g \left(\frac{1}{T_c} - \frac{1}{T_{c,STC}} \right) / K_a} \tag{3}$$

where I_{rs} is the reverse saturation current at STC conditions, E_g is the band-gap energy of the material. In this work for R_s and R_{sh} the same relations in [34] are used as (4) and (5).

$$R_{sh} = R_{sh,STC} \frac{G}{G_{STC}} \tag{4}$$

$$R_s = R_{s,STC} \tag{5}$$

where $R_{s,STC}$ and $R_{sh,STC}$ are the serial resistance and parallel resistance at STC conditions, respectively.

In (1) is valid for a solar cell. For the exact application of this equation for PV module, the term of $(V + R_s I)$ is replaced by $\frac{(V + N_s R_s I)}{N_s}$. To determine the five parameters exist in (1), which are: I_{ph} , R_s , R_{sh} , I_0 and a , you can see [35, 36]. Typically N_s cells are connected in series to get the requisite voltage of PV module. All the cells are forced to carry the same current called panel current in series panel. In this work, actual module was utilised, Shell Solar S75. The electrical parameters of the module under STC form manufacturer are listed in Table 1.

Table 1. Data of experimental PV modules

Silicon type	Shell solar S75
Open circuit voltage (V_{oc})	21.6 V
Short-circuit current (I_{sc})	4.7 A
Maximal voltage (V_{mp})	17.6 V
Maximal current (I_{mp})	4.26 A
Maximal power (P_{mp})	75 W
Number of cells (N_s)	36

Figure 2 shows the simulated and experimental results of the module under different irradiation and temperature levels. The current-voltage (I-V) and power-voltage (P-V) characteristics are shown in Figure 2. Figure 3 revealed the simulation structure of the closed loop system for MATLAB and Simulink, which includes the electrical schema of a one diode model of the PV panel. More details can be found in [37].

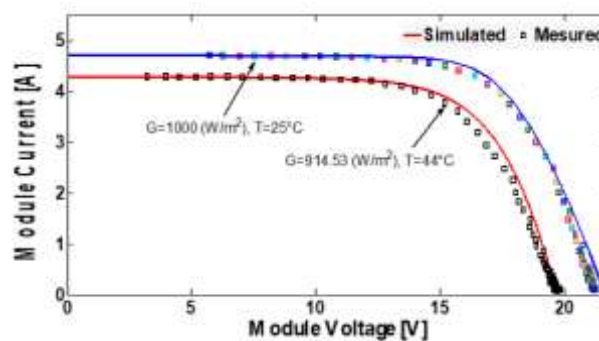


Figure 2. Simulation and experimental results on the test setup

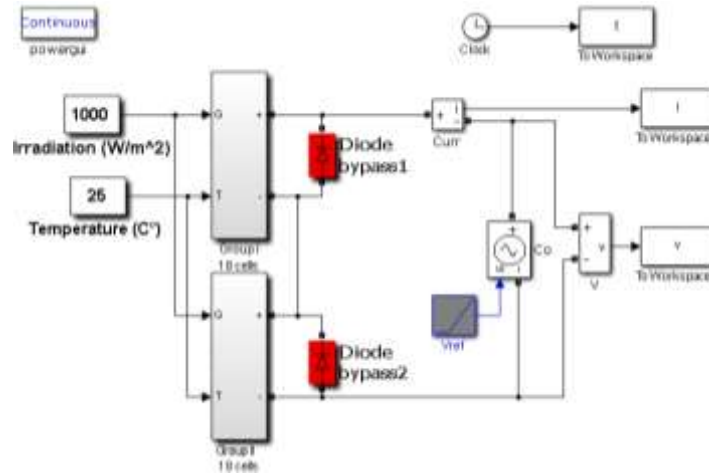


Figure 3. Simulink simulations to illustrate the I-V and P-V module output characteristics

2.1.2. Dynamic model of DC/DC boost converter

In order to force the PV panel functions at the MPPT, we present the principle of the DC-DC boost converter. This type of converter use inductors and capacitors to control the energy flow the PV module to load by continuously opening and closing a switch (K) [38]. The switch is generally an electronic device (Mosfet or IGBT transistor). It is driven by a pulse width modulation (PWW) signal with a fixed frequency and an adjustable duty cycle D (0<D<1). Figure 4 shows a DC-DC boost converter. The relation between the output voltage and input voltage in DC-DC boost converter is given by (6):

$$V_0 = \frac{1}{1-D} V_{pv} \tag{6}$$

the dynamic of the boost converter is given by:

$$\begin{cases} C_1 \frac{dV_{pv}}{dt} = I_{pv} - I_L \\ L \frac{dI_L}{dt} = V_{pv} - (1 - D)V_0 \\ C_2 \frac{dV_0}{dt} = -I_0 + (1 - D)I_L \end{cases} \tag{7}$$

where V_{pv} and I_{pv} : are the voltage and current of the PV module, I_L : the inductor current of the DC-DC converter. V_0 : the DC-DC converter output voltage, D: the duty cycle, L: the filter inductor, C_1 and C_2 : the filter capacitor, R: the nominal resistance of load.

By combing the different equations describing the system [29], global dynamic model can be written as follows:

$$\begin{cases} I = I_{ph} - I_0 \left[e^{\left(\frac{V+I N_s R_s}{V_t N_s}\right)} - 1 \right] - \frac{V+I N_s R_s}{N_s R_{sh}} \\ \frac{dV_{pv}}{dt} = \frac{I_{pv}}{C_1} - \frac{I_L}{C_1} \\ \frac{dV_{pv}}{dt} = \frac{V_{pv}}{L} - \frac{(1-D)}{L} V_0 \\ \frac{dV_0}{dt} = -\frac{I_0}{C_2} + \frac{(1-D)}{C_2} I_L \end{cases} \tag{8}$$

In (8) can be written in compact form of the nonlinear time invariant system;

$$\begin{cases} \dot{X}_1 = \frac{I_{pv}}{C_1} - \frac{1}{C_1} X_2 \\ \dot{X}_2 = \frac{1}{L} X_1 - \frac{u}{L} X_3 \\ \dot{X}_3 = -\frac{1}{RC_2} X_3 + \frac{u}{C_2} X_2 \end{cases} \tag{9}$$

where $X_1 = V_{pv}$; $X_2 = I_L$; $X_3 = V_0$; $u = (1 - D)$; $I_0 = V_0/R$.

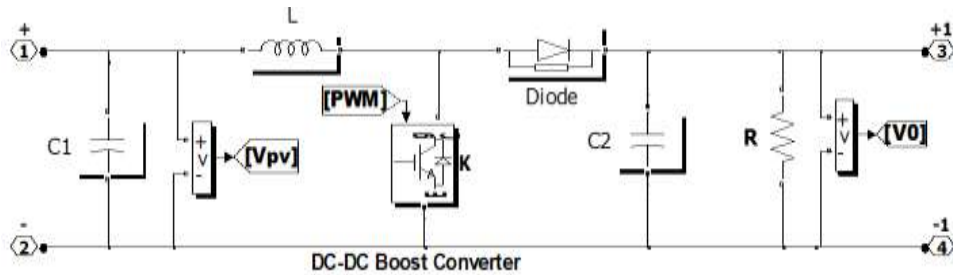


Figure 4. DC-DC boost converter

2.2. Second order sliding mode approach

As the supplied by the photovoltaic energy depends on outdoor conditions, an important account in the design of efficient PV systems is to extract MPP correctly. The purpose of MPPT is to move the output power operating close to the MPP under varying outdoor conditions. The 2-SMC is established for the systems with relative degree two ($r=2$) and does not suffer from chattering while maintaining the robustness of the approach. There are several algorithms to realize 2-SMC in literature. For example, sub-optimal algorithm, the terminal sliding mode algorithm, the twisting algorithm, the super-twisting algorithm. Hence, the STA algorithm is currently preferable over the classical sliding mode control.

2.2.1. Short review of 2-SMC

The SMC consists of two phase: first, we determine a sliding surface $S(X)$ upon which the control objectives are realised. Next, we derive a control law in order to bring the state trajectory to this output and maintain it there at all time [39]. In the situation the difficult is to generate a 2-SM on an appropriately chosen sliding surface and, thus, to constrain the trajectories system to evolve in finite time on $S = \{X: S = \dot{S} = 0\}$. However, the increasing information demand in terms of the first derivative of the sliding surface is the main difficult in the implementation of the 2-SMC, the super twisting sliding mode control scheme is a modified 2-SMC scheme that does not require any knowledge of the derivative of the sliding variable \dot{S} . Consider a system whose dynamics is given by:

$$\begin{aligned} \dot{X} &= f(X,t) + g(X,t)u \\ y &= g(X,t) \end{aligned} \quad (10)$$

where: $X \in \mathcal{R}^n$ is the system state variable, $u \in \mathcal{R}$ is the control, f, g are sufficiently smooth vector fields. $S = S(X, t) \in \mathcal{R}$ is the output function, called sliding variable. By differentiating S with respect to time, t , we have:

$$\ddot{S} = \varphi_A(t, S, \dot{S}) + \vartheta(t, S, \dot{S})\dot{u} \quad (11)$$

The control u is bounded function $|u| \leq U_{\max}$. The dynamics in (11) are assumed to satisfy the following bounding conditions [26]:

$$\begin{aligned} 0 < k_m \leq |\vartheta(t, S, \dot{S})| \leq K_M \\ |\varphi(X, t)| \leq \beta_{ost} \end{aligned} \quad (12)$$

The set $\{t, X, u: |S(t, X)| < S_0\}$ is the linear region, where k_m, K_M and β_{ost} are some positive constants. The algorithm includes two continuous terms that, again, do not depend upon the first time derivative of sliding variable. The algorithm can be defined by the following control law:

$$u_{st} = u_1 + u_2 \quad (13)$$

where

$$\begin{cases} u_1 = -\alpha_1 \text{sign}(S) \\ u_2 = \alpha_2 |S|^\rho \text{sign}(S) \end{cases} \quad (14)$$

with: α_1, α_2 and ρ verifying the following inequality [27] and [40]:

$$\begin{cases} \alpha_1 = \frac{\beta_{ost}}{k_m} \\ \alpha_2^2 = \frac{4\beta_{ost}k_m(\alpha_1 + \beta_{ost})}{K_M^2 k_m(\alpha_1 - \beta_{ost})} \\ 0 < \rho \leq 0 \end{cases} \quad (15)$$

The choice $\rho = 0.5$ ensures that the maximal possible for 2-sliding mode control realization real sliding order two is achieved. Using 2-SMC assures the finite time convergence.

2.2.2. Robust 2-SMC MPPT control approach

In this work the STA has been designed to search MPP. The super twisting algorithm is established for the system with relative degree one so as to reduce the chattering [31]. To make sure that the system states will hit the sliding surface and provides the MPP output, we choose the sliding surface as given in [19]. The state (9) can be expressed by:

$$\begin{aligned} \dot{X} &= f(X,t) + g(X,t)u \\ s(X,t) &= \frac{\partial P_{pv}}{\partial V_{pv}} \end{aligned} \quad (16)$$

where $X = [I_{pv} \quad V_0]^T$, $u = [0 \quad 1]$. The sliding mode surface $S(t)$ is defined as:

$$S(X, t) = \frac{\partial P_{pv}}{\partial V_{pv}} = I_{pv} + V_{pv} \frac{\partial I_{pv}}{\partial V_{pv}} = 0 \quad (17)$$

If we differentiate the sliding surface S , we can write [29]:

$$\dot{S} = \varphi_A(t, S, \dot{S}) + \varnothing(t, S, \dot{S})\dot{u} \quad (18)$$

with

$$\varphi_A(t, S, \dot{S}) = \left(\frac{\partial^3 P_{pv}}{\partial V_{pv}^3} \right) \left(\frac{\partial V_{pv}}{\partial t} \right)^2 + \frac{1}{c_1} \left(\frac{\partial^2 P_{pv}}{\partial V_{pv}^2} \right) \left[\left(\frac{\partial I_{pv}}{\partial V_{pv}} \right) \left(\frac{\partial V_{pv}}{\partial t} \right) - \frac{V_{pv}}{L} \right] \quad (19)$$

$$\varnothing(t, S, \dot{S}) = \frac{1}{c_1} \left(\frac{\partial^2 P_{pv}}{\partial V_{pv}^2} \right) \frac{V_0}{L} \quad (20)$$

where

$$\begin{aligned} \frac{\partial^2 P_{pv}}{\partial V_{pv}^2} &= 2 \frac{\partial I_{pv}}{\partial V_{pv}} + V_{pv} \frac{\partial^2 I_{pv}}{\partial V_{pv}^2} \\ \frac{\partial^3 P_{pv}}{\partial V_{pv}^3} &= 3 \frac{\partial^2 I_{pv}}{\partial V_{pv}^2} + V_{pv} \frac{\partial^3 I_{pv}}{\partial V_{pv}^3} \end{aligned} \quad (21)$$

The control of the boost converter is a bounded function ($0 < u < 1$). We assume that the (18) satisfy condition in (15), the control law guarantees the finite time convergence. The proof of the control law algorithm approach is presented in the appendix. We can consider the applied control law and D can be deduced from the equation $u=1-D$, it is guaranteed that the system state will hit the surface and produce maximum power output persistently.

3. RESULTS AND DISCUSSION

The structure of the closed loop system for MATLAB and Simulink, is shown in Figure 5, which includes the electrical circuit of the photovoltaic module Shell Solar S75, whose characteristics are shown in Table 1, the DC-DC converter BOOST work with $L=130\text{mH}$, $C_1=1000\mu\text{F}$ and $C_2=500\mu\text{F}$, load $R=20\Omega$ and the MPPT algorithm. The switching frequency of the boost converter is set to 25 KHz. The controller parameters are set to $\alpha_1=0.27$ and $\alpha_2=0.05$. The proposed MPPT control is evaluated from three cases including fixed irradiation, varying irradiation and temperature. Furthermore, for the sake of comparison, responses obtained with 2-SMC based on super twisting algorithm (STA) are compared with ones resulting from the 1-SMC (fixed irradiation).

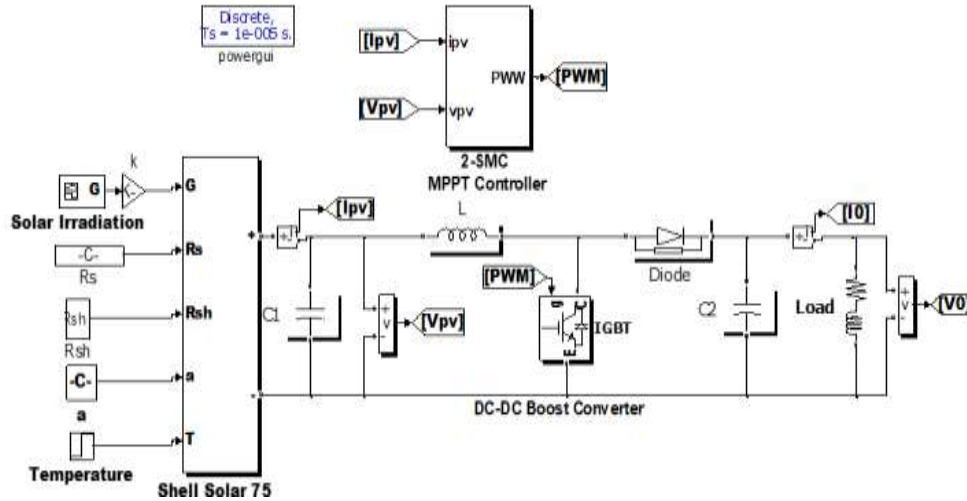


Figure 5. Simulink structure of the closed loop control of boost converter

3.1. Standard test conditions: T=25°C and G=1000 W/m²

Figure 6 (a) displays the waveforms of P_{pv} , V_{pv} , V_0 , I_{pv} and D with the 1-SMC as an MPPT Controller. Figure 7 (a) and displays the waveforms of P_{pv} , V_{pv} , V_0 , I_{pv} and D with the 2-SMC based on STA as an MPPT controller, so that the MPP is located at a power of 75.02 W. It is easily from the below results seen that the system reaches that PV module power and shows a fast response and a good tracking performance. It only takes milliseconds to track MPP. When the MPP is reached, the sliding surface converges to zero Figure 7 (b).

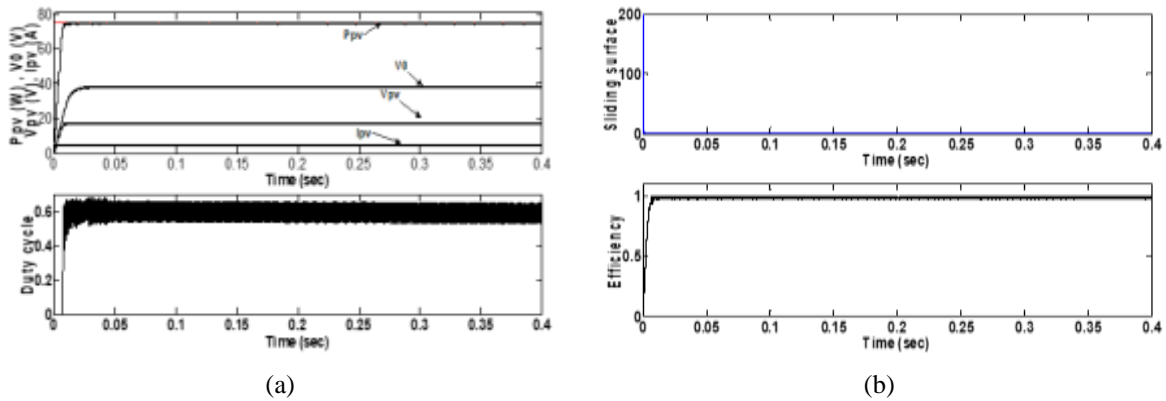


Figure 6. Simulation responses (constant solar irradiation and constant temperature) using 1-SMC

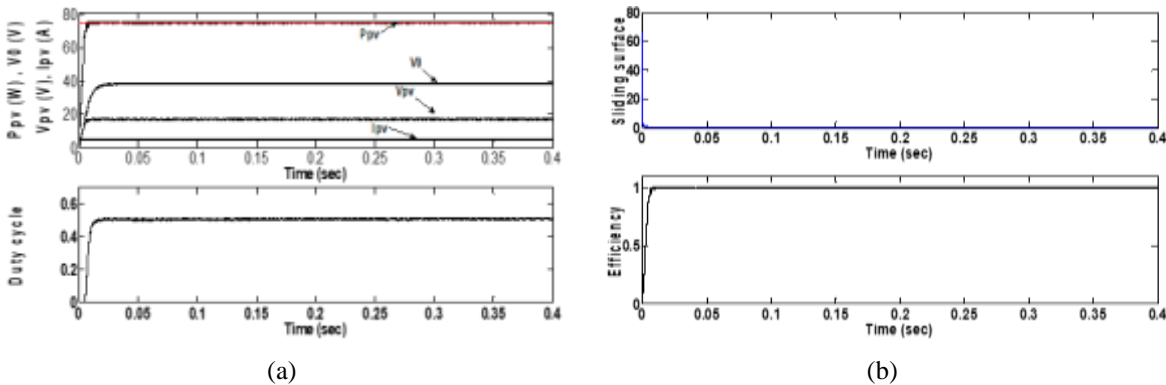


Figure 7. Simulation responses (constant solar irradiation and constant temperature) using 2-SMC

The simulation characteristic curves results (2-SMC) of the photovoltaic system are presented in Figure 8. Figure 9 shows the comparison between PV output power, duty cycle of 2-SMC and 1-SMC as an MPPT controllers tracker. The 2-SMC presents less oscillation than the 1-SMC and which imply good conversion efficiency. All these results prove the effectiveness of our STA control.

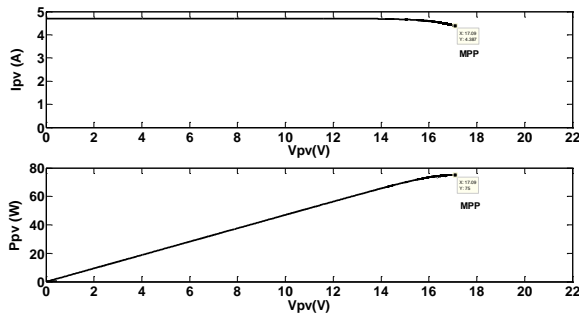


Figure 8. Simulation results of the PV system (I-V and P-V)

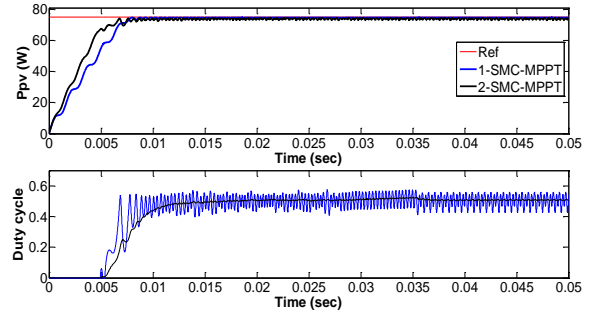


Figure 9. Comparison between PV output power and duty cycle of 2-SMC and 1-SMC based MPP Controllers trackers

3.2. Varying solar irradiation test

Figure 10 (a) shows the tracking results with step irradiance input from 500 W/m² to 800 W/m² at 0.4s and 800 W/m² to 1000 W/m² at 0.6s, while the temperature is constant equal to T=25°C and load R=20Ω. The system reaches steady state of irradiance levels within milliseconds and can track the desired behavior of the MPP rapidly Figure 10 (a) and with less oscillation which implies good conversion efficiency Figure 10 (b).

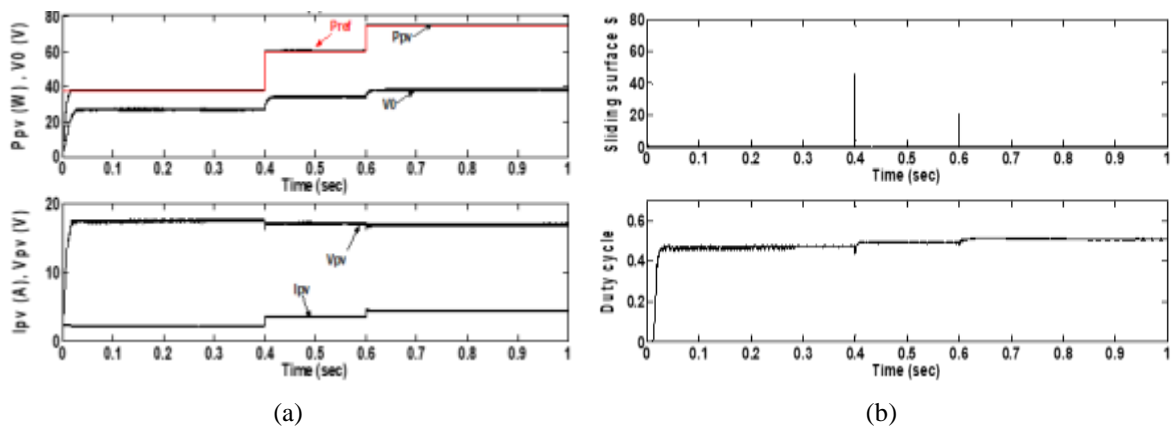


Figure 10. Simulation responses (variable solar irradiation and constant temperature)

3.3. Varying temperature

Figure 11 shows the tracking results with step temperature input from 25°C to 50°C at 0.4s, while the irradiance is constant equal to 1000 W/m² and load R=20Ω. The controller reaches steady state of both temperature levels within small time transit response.

3.4. Experimental results

The basic structure of the laboratory setup (LSP-IE laboratory, University of Batna 2) is illustrated in Figure 12. The Resistance is used as a load. The emulator connected with a boost converter has been used instead of the module. The dSPACE DS1104 PPC is plugged in the host PC. The sensors used for the currents and voltages measure are respectively LA-25NP and LV-25P. The MPPT control law has been implemented in a dSPACE DS1104 R&D controller board. Then the PWM unit directly generates a 25 KHz PWM signal to control IGBT switch of the boost converter. The experimental characteristics of the photovoltaic emulator are shown in Figure 13.

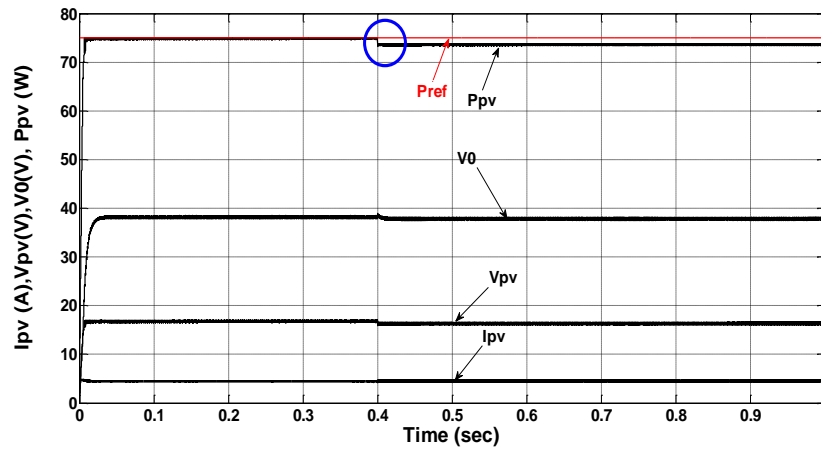


Figure 11. Simulation results of the PV system (constant solar irradiation and variable temperature)

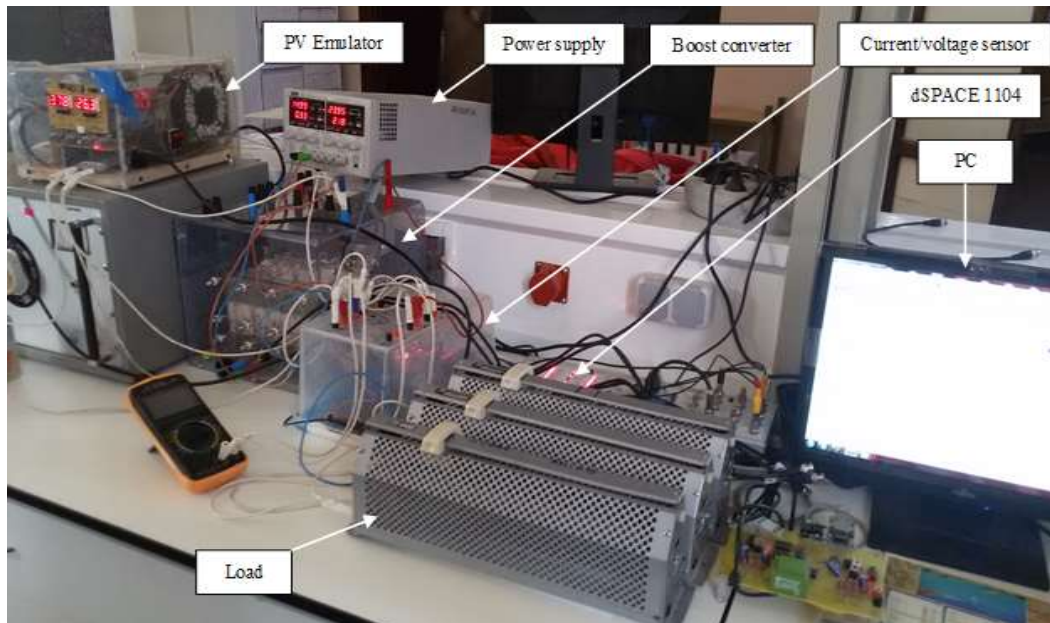


Figure 12. Structure of the laboratory setup

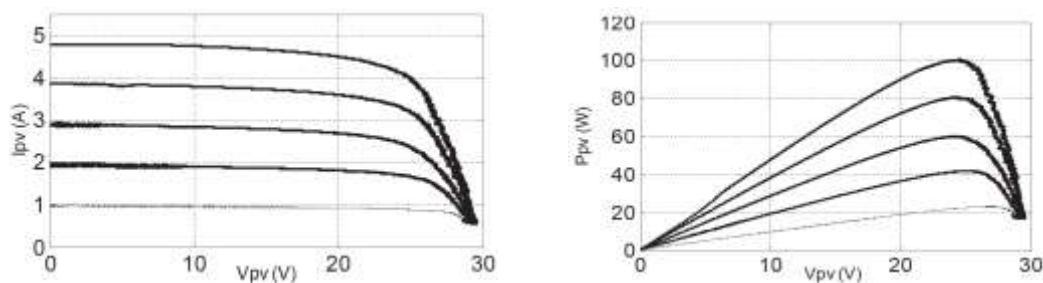


Figure 13. Experimental results of the PV emulator (I-V and P-V) with irradiation [200, 400, 600, 800, 1000] W/m²

The performance and robustness of the MPPT algorithm is evaluated by two experiments:

- Under fixe values of irradiation ($G=1000 \text{ W/m}^2$) and Temperature ($T=25^\circ\text{C}$).
- Under varying irradiation from 500 W/m^2 to 1000 W/m^2 and $T=25^\circ\text{C}$.

The results as shown in Figure 14 demonstrate that the 2-SMC method has good dynamic response and can track the desired behaviour of the MPP power (100 W) well. The 2-SMC is proving robustness against irradiation variation shown in Figure 15.

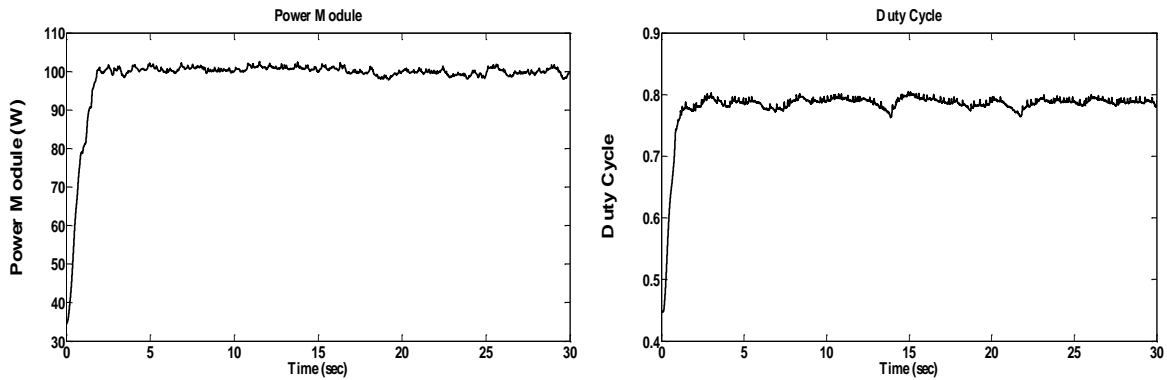


Figure 14. Experimental results of 2-SMC under fixe value of irradiation and temperature

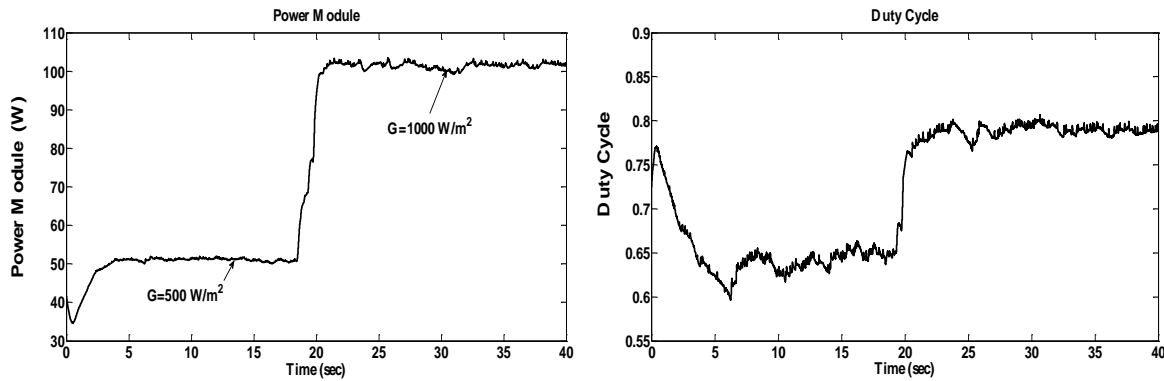


Figure 15. Experimental results of 2-SMC under varying value of irradiation and fixe temperature value

4. CONCLUSION

In this work a robust MPPT control is proposed for the PV application. The proposed controller is capable to track the MPP under different operating conditions. This approach guarantees high dynamic system performances and higher efficiency compared to other algorithms. The robustness against change in irradiation of the proposed method is improved via simulation under MATLAB/Simulink. Also the proposed algorithm offers a solution to eliminate the chattering phenomenon. This approach is the foundation of a practical implementation follow-up this research work. The effectiveness and the feasibility of the improved 2-SMC was verified by experiments

APPENDIX

Proof. In order to demonstrate the stable convergence property of the proposed approach [41]:

$$S(X, t) = \frac{\partial P_{pv}}{\partial V_{pv}} \tag{A.1}$$

If $S(X,t)$ is made equal to zero ,then the maximal power is taken. The controller steer the derivative S to zero, by action on the duty cycle u . We can write:

$$S(X, t) = \frac{\partial P_{pv}}{\partial V_{pv}} = I_{pv} + V_{pv} \frac{\partial I_{pv}}{\partial V_{pv}} = 0 \tag{A.2}$$

In view of (1) and $R_s, R_{sh}=\infty$, its dynamics is given by:

$$\dot{S} = -\frac{I_0}{V_t C_1} e^{\frac{V_{pv}}{V_t}} \left(2 + \frac{V_{pv}}{V_t}\right) (I_{pv} - I_L) \quad (A.3)$$

The second derivative of S is described by the following (A.4):

$$\ddot{S} = -\frac{I_0}{V_t C_1} \left[\frac{1}{V_t C_1} \left(3 + \frac{V_{pv}}{V_t}\right) (I_{pv} - I_L)^2 + \left(2 + \frac{V_{pv}}{V_t}\right) \left(\frac{dI_{pv}}{dt} - \dot{I}_L\right) \right] \quad (A.4)$$

As shown in (A.4) can be rewritten as follows:

$$\ddot{S} = \varphi_A(t, S, \dot{S}) + \vartheta(t, S, \dot{S})u \quad (A.5)$$

where

$$\varphi_A(t, S, \dot{S}) = -\frac{I_0}{V_t C_1} e^{\frac{V_{pv}}{V_t}} \left[\frac{A}{C_1} \left(3 + \frac{V_{pv}}{V_t}\right) (I_{pv} - I_L)^2 + \left(2 + \frac{V_{pv}}{V_t}\right) \left(\frac{dI_{pv}}{dt} - \frac{1}{L}(V_{pv} - V_0)\right) \right] \quad (A.6)$$

$$\vartheta(t, S, \dot{S}) = \frac{I_0}{V_t L C_1} \left(2 + \frac{V_{pv}}{V_t} V_0\right) e^{\frac{V_{pv}}{V_t}} \quad (A.7)$$

As shown in (A.5) has the relative degree two with respect to the input u .

ACKNOWLEDGEMENTS

This project was financially supported by the Directorate General for Scientific Research and Technological Development-Algerian Ministry of Higher Education and Scientific Research.

REFERENCES

- [1] K. Kraatz and A. Zahedi, "Energy management and control strategies of electric vehicle integrated into the smart grid," *2015 Australasian Universities Power Engineering Conference (AUPEC)*, Wollongong, NSW, pp. 1-5, 2015.
- [2] K. Sundareswaran, S. Peddapati and S. Palani, "MPPT of PV Systems Under Partial Shaded Conditions Through a Colony of Flashing Fireflies," in *IEEE Transactions on Energy Conversion*, vol. 29, no. 2, pp. 463-472, 2014.
- [3] S. Nema, R. K. Nema and G. Agnihotri, "MATLAB/Simulink based study of photovoltaic cells/modules/array and their experimental verification," *International Journal of Energy and environment*, vol. 1, no. 3, pp. 487-500, 2010.
- [4] C. Dorofte, U. Borup and F. Blaabjerg, "A combined two-method MPPT control scheme for grid-connected photovoltaic systems," *2005 European Conference on Power Electronics and Applications*, Dresden, pp. 10, 2005.
- [5] S. Dhar, R. Sridhar and G. Mathew, "Implementation of PV cell based standalone solar power system employing incremental conductance MPPT algorithm," *2013 International Conference on Circuits, Power and Computing Technologies (ICCPCT)*, Nagercoil, pp. 356-361, 2013.
- [6] A. Safari and S. Mekhilef, "Simulation and Hardware Implementation of Incremental Conductance MPPT With Direct Control Method Using Cuk Converter," in *IEEE Transactions on Industrial Electronics*, vol. 58, no. 4, pp. 1154-1161, 2011.
- [7] A. K. Abdelsalam, A. M. Massoud, S. Ahmed and P. N. Enjeti, "High-Performance Adaptive Perturb and Observe MPPT Technique for Photovoltaic-Based Microgrids," in *IEEE Transactions on Power Electronics*, vol. 26, no. 4, pp. 1010-1021, 2011.
- [8] S. M. R. Kazmi, H. Goto, O. Ichinokura and H. Guo, "An improved and very efficient MPPT controller for PV systems subjected to rapidly varying atmospheric conditions and partial shading," *2009 Australasian Universities Power Engineering Conference*, Adelaide, SA, pp. 1-6, 2009.
- [9] P. Sivakumar, A. Abdul Kader, Y. Kaliavaradhan and M. Arutchelvi, "Analysis and enhancement of PV efficiency with incremental conductance MPPT technique under non-linear loading conditions," *Renewable Energy*, vol. 81, pp. 543-550, 2015.
- [10] A. K. Rai, N. D. Kaushika, B. Singh and N. Agarwal, "Simulation model of ANN based maximum power point tracking controller for solar PV system," *Solar Energy Materials and Solar Cells*, vol. 95, no. 2, pp. 773-778, 2011.
- [11] L. Letting, J. Munda and Y. Hamam, "Optimization of a fuzzy logic controller for PV grid inverter control using s-function based PSO," *Solar Energy*, vol. 86, no. 6, pp. 1689-1700, 2012.
- [12] Y. Chen, Y. Jhang and R. Liang, "A fuzzy-logic based auto-scaling variable step-size MPPT method for PV systems," *Solar Energy*, vol. 126, pp. 53-63, 2016.
- [13] A. Khiareddine, C. B. Salah and M. F. Mimouni, "Power management of a photovoltaic/battery pumping system in agricultural experiment station," *Solar Energy*, vol. 112, pp. 319-338, 2015.

- [14] Y. Gheddadi, F. Errahimi and E. Najja, "Design and verification of photovoltaic MPPT algorithm as an automotive-based embedded software," *Solar Energy*, vol. 171, pp. 414-425, 2018.
- [15] V. Utkin, "Variable structure systems with sliding modes," in *IEEE Transactions on Automatic Control*, vol. 22, no. 2, pp. 212-222, 1977.
- [16] H. De Battista and R. J. Mantz, "Variable structure control of a photovoltaic energy converter," in *IEE Proceedings - Control Theory and Applications*, vol. 149, no. 4, pp. 303-310, 2002.
- [17] E. Mamarelis, G. Petrone and G. Spagnuolo, "Design of a Sliding-Mode-Controlled SEPIC for PV MPPT Applications," in *IEEE Transactions on Industrial Electronics*, vol. 61, no. 7, pp. 3387-3398, 2014.
- [18] M. R. Mojallizadeh, M. A. Badamchizadeh, S. Khanmohammadi and M. Sabahi, "Designing a new robust sliding mode controller for maximum power point tracking of photovoltaic cells," *Solar Energy*, vol. 132, pp. 538-546, 2016.
- [19] C. S. Chiu, Y. L. Ouyang, and C. Y. Ku, "Terminal sliding mode control for maximum power point tracking of photovoltaic power generation systems," *Solar energy*, vol. 86, no. 10, pp. 2986-2995, 2012.
- [20] C-C. Chu and C-L. Chen, "Robust maximum power point tracking method for photovoltaic cells: A sliding mode control approach," *Solar Energy*, vol. 83, no. 8, pp. 1370-1378, 2009.
- [21] V. I. Utkin, "Sliding mode control design principles and applications to electric drives," in *IEEE Transactions on Industrial Electronics*, vol. 40, no. 1, pp. 23-36, 1993.
- [22] V. I. Utkin, "Sliding modes in control and optimization," Germany: Springer-Verlag Berlin Heidelberg, 1992.
- [23] I. Utkin, J. Gulder and J. Shi, "Sliding mode control in electromechanical systems," United Kingdom: *CRC Press*, 1999.
- [24] K. D. Young, V. I. Utkin and U. Ozguner, "A control engineer's guide to sliding mode control," in *IEEE Transactions on Control Systems Technology*, vol. 7, no. 3, pp. 328-342, 1999.
- [25] A. G. Bondarev, S. A. Bondarev, N. E. Kostyleva, and V. I. Utkin, "Sliding modes in systems with asymptotic state observers," *Automatika I Telemekhanika*, vol. 46, no. 6, pp. 679-684, 1985.
- [26] G. Bartolini, A. Ferrara, A. Levant, and E. Usai, "On second order sliding mode controllers," *Variable Structure Systems, Sliding Mode and Nonlinear Control*, vol. 247, pp. 329-350, 2007.
- [27] A. Levant, "Sliding order and sliding accuracy in sliding mode control," *International Journal of Control*, vol. 58, no. 6, pp. 1247-1263, 1993.
- [28] H. Saharaoui, L. Chrifi-Alaoui, S. Drid, and P. Bussy, "Second order sliding mode control of dc-dc converter used in the photovoltaic system according an adaptive MPPT," *International Journal of Renewable Energy Research*, vol. 6, no. 2, pp. 475-383, 2016.
- [29] H. Yatimi and E. Aroudam, "Assessment and control of a photovoltaic energy storage system based on the robust sliding mode MPPT controller," *Solar Energy*, vol. 139, pp. 557-568, 2016.
- [30] M. R. Mojallizadeh and M. A. Badamchizadeh, "Second-order fuzzy sliding-mode control of photovoltaic power generation systems," *Solar Energy*, vol. 149, pp. 332-340, 2017.
- [31] A. Kchaou, A. Naamane, Y. Koubaa, and N. M'sirdi, "Second order sliding mode-based MPPT control for photovoltaic applications," *Solar Energy*, vol. 155, pp. 758-769, 2017.
- [32] H. Patel and V. Agarwal, "MATLAB-Based Modeling to Study the Effects of Partial Shading on PV Array Characteristics," in *IEEE Transactions on Energy Conversion*, vol. 23, no. 1, pp. 302-310, 2008.
- [33] M. U. Siddiqui, A. F. M. Arif, A. M. Bilton, S. Dubowsky, and M. Elshafei, "An improved electric circuit model for photovoltaic modules based on sensitivity analysis," *Solar Energy*, vol. 90, pp. 29-42, 2013.
- [34] W. D. Soto, S. A. Klein, and W. A. Beckam, "Improvement and validation of a model for photovoltaic array performance," *Solar Energy*, vol. 80, no. 1, pp. 78-88, 2006.
- [35] A. Fezzani, I. Hadj-Mahammed, S. Drid, A. Bouchakour, L. Zaghba, M. Benbitour and H. S. Oudjana, "Degradation evaluation of PV module using solmetric PVA-600 analyzer," *The 4th International Seminar on New and Renewable Energies (SIENR'2016)*, Ghardaia, 2016.
- [36] A. Fezzani, I. Hadj-Mahammed, S. Drid, L. Zaghba, A. Bouchakour, and M. Benbitour, "Degradation and performance evaluation of PV module in desert climate conditions with estimate uncertainty in measuring," *Serbian Journal of Electrical Engineering*, vol. 14, no. 2, pp. 277-299, 2017.
- [37] A. Fezzani, I. Hadj-Mahammed, S. Drid, and L. Chrifi-Alaoui, "Modelling and analysis of the photovoltaic array faults," *2015 3rd International Conference on Control, Engineering & Information Technology (CEIT)*, Tlemcen, pp. 1-9, 2015.
- [38] Jingquan Chen, R. Erickson and D. Maksimovic, "Averaged switch modeling of boundary conduction mode DC-to-DC converters," *IECON'01. 27th Annual Conference of the IEEE Industrial Electronics Society (Cat. No.37243)*, Denver, CO, USA, vol. 2, pp. 844-849, 2001.
- [39] M. Djemai, K. Bosawon, Benmonsour, and A. Marouf, "High-order sliding mode control of a DC drive via a switched controller multicellular converter," *International Journal of Systems Science*, vol. 42, no. 11, pp. 1869-1888, 2011.
- [40] S. V. Emelyanov, S. K. Korovin, and L. V. Levantovsky, "Higher order sliding regimes in the binary control systems," *Soviet Physics Doklady*, vol. 31, pp. 291-293, 1986.
- [41] O. E. L. Maguire, A. Farchi, and E. M. Louragli, "Sliding mode control approach for maximum power tracking in single-phase grid-connected photovoltaic systems," *IOSR Journal of Electrical And Electronics Engineering (IOSR-JEEE)*, vol. 9, no. 4, pp. 41-49, 2014.

BIOGRAPHIES OF AUTHORS

Amor Fezzani was born in Batna (Algeria), on September 9, 1971. He graduated from the El Hadj Lakhda. University (Algeria) in 1996 with electrical engineering degree. He received M.Sc. and Ph.D degrees in electrical engineering, from the University of Batna, Algeria, respectively in 2009 and 2015. Currently, he is researcher at the Unité de Recherche Appliquée en Energies Renouvelables, URAER, Centre de Développement des Energies Renouvelables, CDER, Alegria. His research interests concern: renewable energy, power electronics, electric machines, robust control, etc.



Noureddine Bouarroudj was born in Cheria, Tebessa, Algeria, in 1983. He received his degree in Automatic control from the University of Tebessa, Algeria, in 2008 and his MSc, and Ph.D degrees in electrical engineering (automatic option) from Ecole Nationale Polytechnique (ENP), Algeria, respectively in 2011, and 2017. He is currently a Researcher in Unité de Recherche Appliquée en Energies Renouvelables/CDER, Ghardaia, Algeria. His research interests include fractional-order control, sliding mode control, renewable energy systems and their controls and control optimisation.



Said Drid was born in Batna, Algeria, in 1969. He received B.Sc., M.Sc. and PhD degrees in electrical engineering, from the University of Batna, Algeria, respectively in 1994, 2000 and 2005. Currently, he is full professor at the Electrical Engineering Institute at University of Batna, Algeria. He is the head of the “Energy Saving and Renewable Energy” team in the Research Laboratory of Electromagnetic Induction and Propulsion Systems of Batna University. He is currently the vice chair of the PES chapter, IEEE Algeria subsection. His research interests include electric machines and drives, renewable energy, field theory and computational electromagnetism.



Layachi Zaghba received his diploma degree in Automatic Engineering in 2002 and his MSc degree in electronics in 2005 from the Science and Technology, Department of Jijel University. He received his PhD degree in electrical engineering (automatic) from the University of Biskra, Algeria, in 2017. Now, He is a researcher at the Unit for Applied Research in Renewable Energy (URAER), Ghardaia, Algeria. His main interest areas are the photovoltaic systems and their applications, control, optimization, performance analysis of grid connected photovoltaic.